

Theoretical review of diffractive phenomena

K. Golec-Biernat ^a

^aH. Niewodniczański Institute of Nuclear Physics, Polish Academy of Sciences
31-342 Cracow, Poland

We review QCD based descriptions of diffractive deep inelastic scattering emphasising the role of models with parton saturation. These models provide natural explanation of such experimentally observed facts as the constant ratio of $\sigma^{diff}/\sigma^{tot}$ as a function of the Bjorken variable x , and Regge factorization of diffractive parton distributions. The Ingelman-Schlein model and the soft color interaction model are also presented.

1. Introduction

One of the most important experimental results from the DESY ep collider HERA is the observation of a significant fraction (around 10%) of diffractive events in deep inelastic scattering (DIS) with large rapidity gap between the scattered proton, which remains intact, and the rest of the final system [1, 2, 3]. In the standard, QCD description of DIS such events are not expected in such an abundance since large gaps are exponentially suppressed due to color strings formed between the proton remnant and scattered partons. For diffractive events, however, a color neutral cluster of partons fragments independently of the scattered proton. The ratio of diffractive to all DIS events depends weakly on the Bjorken variable x and photon virtuality Q^2 . Thus, DIS diffraction is a leading twist effect with logarithmic scaling violation in Q^2 . The theoretical description of diffractive events is a real challenge since it must combine perturbative QCD effect of hard scattering with nonperturbative phenomenon of rapidity gap formation. It would be also desirable to apply this description to analogous diffractive phenomena in hadronic collisions with hard jets separated in rapidity from (one or two) unshattered hadrons. Actually, hard diffraction was observed for the first time in $p\bar{p}$ scattering by UA8 collaboration [4].

In this presentation we concentrate on the discussion of theory of hard diffraction, when there exists a hard scale, the photon virtuality Q^2 or jet transverse momentum, which allows to apply perturbative QCD. Soft diffraction, when such a scale is missing, is outside the scope of our review. The reason being no significant progress in the development of new theoretical ideas concerning soft diffraction since the seventies, in addition to the existing ones based on the Regge pole phenomenology. This phenomenology, however, turns out to be quite useful in the description of a soft part of hard diffraction, responsible for the rapidity gap formation.

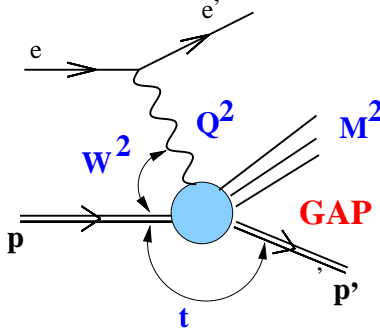


Figure 1. *Kinematic invariants in DIS diffraction in electron–proton collision.*

2. Diffractive parton distributions

Let us start with a brief description of kinematical variables in DIS diffraction, shown in Fig. 1. In addition to the photon virtuality Q^2 and total energy of the γ^*p system W , there are two additional invariant variables related to the diffractive nature of the process: invariant mass of the diffractive system M^2 and the squared momentum transfer t . The following dimensionless fractions are built out of these variables:

$$x_{\mathcal{P}} = \frac{Q^2 + M^2 - t}{Q^2 + W^2}, \quad (1)$$

which is a fraction of the incident proton momentum transferred into the diffractive system, and

$$\beta = \frac{Q^2}{Q^2 + M^2 - t}, \quad (2)$$

being an analogue of the Bjorken variable x for the diffractive system. Experimentally $|t| \ll Q^2, M^2$, thus t can be neglected in the above formulas. Finally, the Bjorken variable

$$x = \frac{Q^2}{Q^2 + W^2} = \beta x_{\mathcal{P}}. \quad (3)$$

After averaging over the azimuthal angle of the scattered proton, the diffractive cross section is characterized by two dimensionful *diffractive structure functions* $F_{2,L}^{D(4)}$

$$\frac{d^4\sigma^D}{dx dQ^2 dx_{\mathcal{P}} dt} = \frac{2\pi\alpha_{em}^2}{x Q^4} \left\{ [1 + (1-y)^2] F_2^{D(4)} - y^2 F_L^{D(4)} \right\}, \quad (4)$$

in a full analogy to inclusive DIS. They depend on four variables: $(x, Q^2; x_{\mathcal{P}}, t)$. After the integration over t (if t is not measured), the dimensionless structure functions are obtained. Due to the kinematical factor in (4), we neglect the longitudinal structure function $F_L^{D(4)}$ in the following.

The leading twist description of diffractive DIS is realized using *diffractive parton distributions* (DPD) q_i^D , where i enumerates quark flavour, in terms of which

$$F_2^{D(4)} = \sum_{i=1}^{N_f} e_i^2 \beta \left\{ q_i^D(x_{\mathcal{P}}, t; \beta, Q^2) + \bar{q}_i^D(x_{\mathcal{P}}, t; \beta, Q^2) \right\}, \quad (5)$$

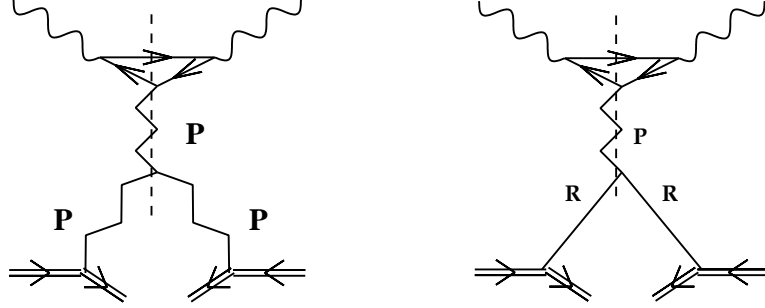


Figure 2. *The pomeron and reggeon contributions to diffractive structure function.*

in the leading logarithmic approximation. In addition to the quark distributions, the gluon DPD $g(x_{\mathcal{P}}, t; \beta, Q^2)$ is also defined. Eq. (5) is an example of the collinear factorization formula proven for DIS diffraction in [5]. In the infinite momentum frame, the DPD have an interpretation of conditional probabilities to find a parton in the proton with the momentum fraction $x = \beta x_{\mathcal{P}}$ under the condition that the incoming proton stays intact and loses the fraction $x_{\mathcal{P}}$ of its momentum. A systematic approach to diffractive parton distributions, based on quark and gluon operators, is given in [8, 9].

The Q^2 -dependence of DPD is governed by the Altarelli-Parisi (DGLAP) evolution equations. In order to find this dependence, initial conditions at some starting scale have to be specified, e.g. from fits to diffractive DIS data in full analogy to the inclusive case [1, 2, 3]. In the evolution equations only (β, Q^2) are relevant variables while $(x_{\mathcal{P}}, t)$ play the role of external parameters. Thus, a modelling of the latter dependence for DPD is necessary. This is done using physical ideas about the nature of interactions leading to DIS diffraction.

Traditionally, diffraction is related to the exchange of a pomeron. This is the dominant at high energy vacuum quantum number exchange, described by a Regge pole with a linear trajectory $\alpha_{\mathcal{P}}(t) = \alpha_{\mathcal{P}}(0) + \alpha' t$ and the intercept $\alpha_{\mathcal{P}}(0) \geq 1$. In the Ingelman-Schlein model [10] of hard diffraction the pomeron exchanged between the proton and diffractive system is supplemented by hard QCD structure with partons. In this case, the DPD factorize into a pomeron flux

$$f(x_{\mathcal{P}}, t) = \frac{B^2(t)}{8\pi^2} x_{\mathcal{P}}^{1-2\alpha_{\mathcal{P}}(t)}, \quad (6)$$

and pomeron parton distributions $q_i^{\mathcal{P}}(\beta, Q^2)$:

$$q_i^D(x_{\mathcal{P}}, t; \beta, Q^2) = f(x_{\mathcal{P}}, t) q_i^{\mathcal{P}}(\beta, Q^2). \quad (7)$$

In the above $B(t)$ is the Dirac electromagnetic form factor of the proton [11], and β is a fraction of the pomeron momentum carried by a struck quark. Since the pomeron carries the vacuum quantum numbers, the pomeron quark and antiquark distributions are equal: $q_i^{\mathcal{P}} = \bar{q}_i^{\mathcal{P}}$. The inspired by the Regge theory factorization (7) is called *Regge factorization*. To good accuracy, this type of factorization was found in the diffractive data at HERA [1, 2].

The QCD analysis of the early diffractive data from HERA, using the Ingelman-Schlein model, was done in [12] with the soft pomeron trajectory $\alpha_{\mathcal{P}}(t) = 1.1 + 0.25 \cdot t$ and

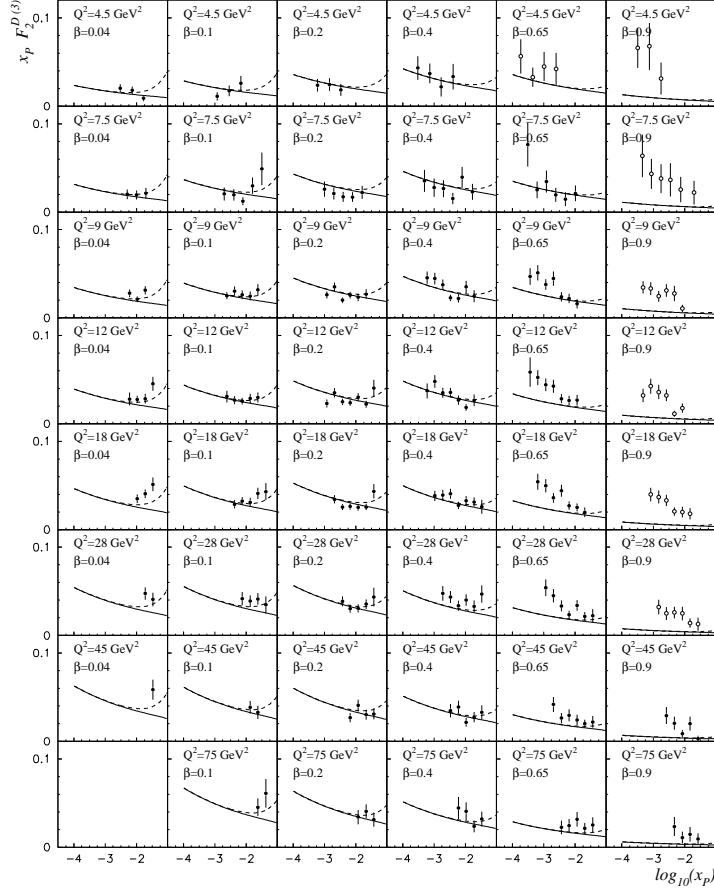


Figure 3. *The pomeron (solid) and reggeon (dashed) contributions to diffractive structure function [13]. The data are from [1].*

parameters of the pomeron parton distributions determined from analyses of soft hadronic reactions. More recent analyses of inclusive DIS diffraction [1, 2, 3] assume Regge form of DPD (7) determined by the DGLAP based fits. In particular, the effective slope $\alpha_{\mathbb{P}}(0) = 1.16$ was found as a result of a fit in the recent analysis [3]. In all cases, the fits give large gluon DPD with the relative contribution to the pomeron momentum around 80 – 90% [1].

The collinear factorization fails in hadron–hadron hard diffractive scattering due to initial state soft interactions [6, 7]. Thus, unlike inclusive scattering, the diffractive parton distributions are no universal quantities. They can be used, however, for different diffractive processes in DIS scattering, e.g. diffractive dijet production, for which the collinear factorization theorem holds.

3. Subleading reggeons

The exchange of subleading reggeons can account for the Regge factorization breaking of diffractive structure function for large values of $x_{\mathbb{P}} > 0.01$. Strictly speaking, we cannot call such processes diffractive since diffraction is usually associated with the leading

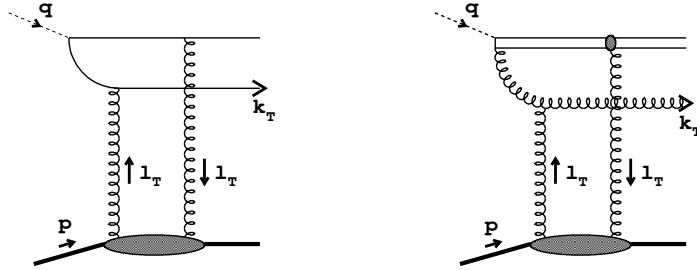


Figure 4. *The $q\bar{q}$ and $q\bar{q}g$ components of the diffractive system.*

pomeron exchange. However, for simplicity we use the same terminology for the non-pomeron exchanges, including the isospin changing process with neutron instead of the proton in the final state. The reggeon contribution is shown in Fig. 2, which illustrates the following extension of the Ingelman-Schlein model [13]

$$F_2^{D(4)}(x, Q^2, x_P, t) = f_P(x_P, t) F_2^P(\beta, Q^2) + \sum_R f_R(x_P, t) F_2^R(\beta, Q^2), \quad (8)$$

where the non-pomeron terms describe reggeon exchanges, isoscalar (f_2, ω) and isovector (a_2, ρ), with the trajectory $\alpha_R(t) = 0.5475 + 1 \cdot t$ in the reggeon fluxes $f_R(x_P, t)$. F_2^R is a reggeon structure function determined in [13]. With such a structure function the Regge factorization is obviously broken for large x_P , which is shown in Fig. 3 by dashed lines.

4. Parton saturation and diffraction

The leading twist DPD lead to good description of data. However, the basic experimental fact that $\sigma^{diff}/\sigma^{tot} \simeq const$ as a function of energy W is not understood in this approach. The understanding is provided in a different theoretical framework of DIS diffraction in which the virtual photon splits into a quark-antiquark pair which subsequently scatters off the target proton through a further quantum fluctuation. This picture is valid in the frame in which the $q\bar{q}$ pair (dipole) carries most of the available rapidity $Y \sim \ln(1/x)$ of the system, and the light-cone photon momentum $q^+ > 0$. The gluon radiation from the parent dipole can be interpreted in the large N_c limit as a collection of dipoles of different transverse sizes which interact with the proton. If the proton stays intact, the diffractive events with large rapidity gap are formed. In such a case, the diffractive system is given by the color dipoles and the pomeron can be modelled by color singlet gluon exchange between the dipoles and the proton.

In the simplest case when only the parent $q\bar{q}$ dipole form a diffractive system, see Fig. 4, the diffractive cross section at $t = 0$ reads [14]

$$\frac{d\sigma^{diff}}{dt} \Big|_{t=0} = \frac{1}{16\pi} \int d^2r dz |\Psi^\gamma(r, z, Q^2)|^2 \hat{\sigma}^2(x, r), \quad (9)$$

where Ψ^γ is the well known light-cone wave function of the virtual photon, r is the dipole transverse size and z is a fraction of the photon momentum q^+ carried by the quark. The *dipole cross section* $\hat{\sigma}(x, r)$ in this formula describes the pomeron interaction, which in the

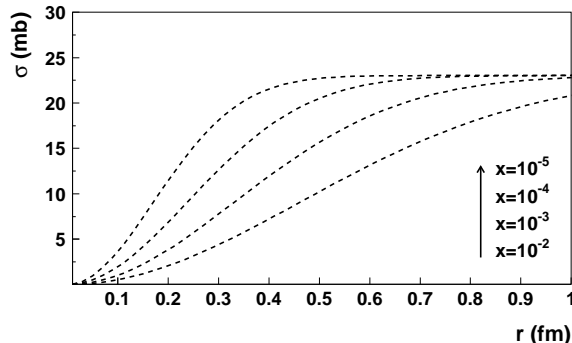


Figure 5. *The dipole cross section (11).*

QCD approach is modelled by the exchange of gluons. The simplest, two gluon exchange does not depend on energy and has to be rejected. Since the DIS diffraction is a typical high energy (small x) phenomenon, it is tempting to apply the BFKL pomeron [15] with two reggeized, interacting gluons. However, the resulting energy dependence is too strong in this case. Thus, more complicated gluon exchanges are necessary.

Particularly important are those [16] which do not lead to the violation of the Froissart unitary bound for the total γ^*p cross section: $\sigma^{tot} \leq c \ln^2 W^2$. Applying the $q\bar{q}$ dipole picture to σ^{tot} , the following relation holds in the small- x limit [14]

$$\sigma^{tot} = \int d^2r dz |\Psi^\gamma(r, z, Q^2)|^2 \hat{\sigma}(x, r), \quad (10)$$

with the same dipole cross $\hat{\sigma}(x, r)$ as in (9). In order to fulfil the Froissart bound, the following phenomenological form of the dipole cross section was proposed in [17]

$$\hat{\sigma}(x, r) = \sigma_0 \{1 - \exp(-r^2 Q_s^2(x))\}, \quad (11)$$

where $Q_s(x) = Q_0 x^{-\lambda}$ is a saturation scale which parameters (together with σ_0) were found from a fit to all small- x data on $\sigma^{tot} \sim F_2/Q^2$. Having obtained the dipole cross section from the analysis of inclusive data, it can be used to predict diffractive cross sections in DIS. This strategy was successfully applied in [18].

Formula (11) captures essential features of parton saturation [16, 20]. For $r \gg 1/Q_s(x)$ the dipole cross section saturates to a constant value σ_0 , which may be regarded as a unitarity bound leading to the behaviour respecting the Froissart condition: $\sigma^{tot} \sim \ln W^2$. For $x \rightarrow 0$ the dipole cross section saturates for smaller dipoles, thus with increasing energy the proton blacken for the dipole probe of fixed transverse size. An important aspect of the form (11), in which r and x are combined into one dimensionless variable $rQ_s(x)$, is geometric scaling, new scaling in inclusive DIS at small x [19]. Qualitatively, the behaviour (11) can be found from an effective theory of dense parton systems with saturation – the Color Glass Condensate, see [20] and reference therein.

The DIS diffraction is an ideal process to study parton saturation since it is especially sensitive to the large dipole contribution, $r > 1/Q_s(x)$. Unlike inclusive DIS, the region below is suppressed by an additional power of $1/Q^2$. The dipole cross section with

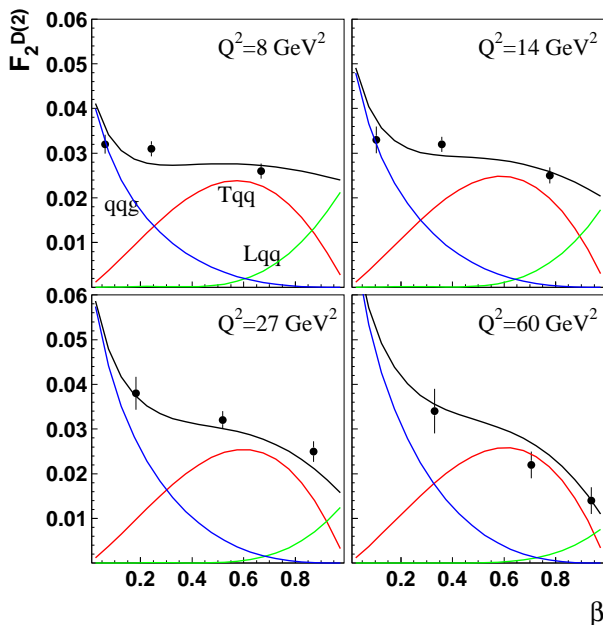


Figure 6. *The diffractive structure function as a function of β at fixed $x_{\mathcal{P}} = 0.003$. Three components of the diffractive system are shown.*

saturation (11) leads in a natural way to the constant ratio (up to logarithms) [17]

$$\frac{\sigma^{diff}}{\sigma^{tot}} \sim \frac{1}{\ln(Q^2/Q_s^2(x))}. \quad (12)$$

In the analysis [18] of DIS diffraction, the dipole cross section (11) was used for the description of the interaction of the diffractive system and the proton. The simplest system, which dominates for diffractive masses $M^2 \sim Q^2$, is formed by the $q\bar{q}$ pair. However, for large diffractive masses, $M^2 \gg Q^2$, the $q\bar{q}g$ component is more important. In Fig. 6 we show the result of the comparison of the saturation model predictions with the ZEUS data [2], indicating three components of the diffractive system: the $q\bar{q}$ state from transverse and longitudinal polarized virtual photon, and $q\bar{q}g$ component. A recent analysis of diffractive data using the same idea but different prescription for the dipole cross section is given in [21].

The high energy formula (9) contains all powers of $1/Q^2$ (twists). Extracting the leading twist contribution from both the $q\bar{q}$ and $q\bar{q}g$ components, the quark and gluon DPD can be directly computed in the saturation model [22]. An exciting aspect of this calculation is the Regge factorization of the DPD,

$$x_{\mathcal{P}} q^D(x_{\mathcal{P}}, \beta) = Q_s^2(x_{\mathcal{P}}) \bar{q}(\beta) \sim x_{\mathcal{P}}^{-0.3}, \quad (13)$$

due to the form (11) with the combined variable $r Q_s$. The dependence: $F_2^D \sim x_{\mathcal{P}}^{1-2\alpha_{\mathcal{P}}}$ with $\alpha_{\mathcal{P}} \approx 1.15$, resulting from (13), is in remarkable agreement with the data [1, 2, 3]. Thus the Regge factorization and the dependence on energy of the diffractive DIS data are naturally explained in the parton saturation approach. This fact emphasize importance of unitarity in the QCD description of DIS diffraction.

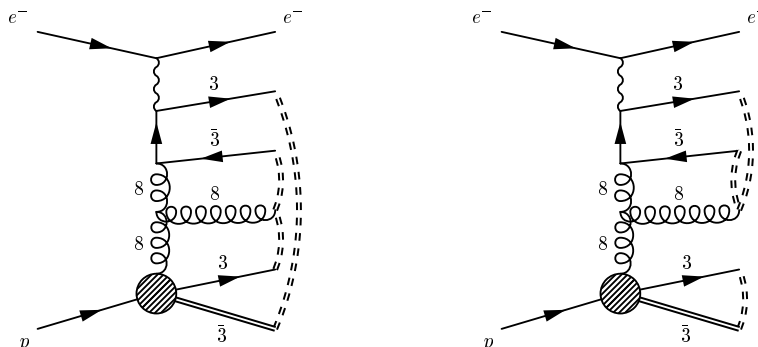


Figure 7. *Typical string configuration in the Lund string model (left) and configuration after the color rearrangement (right).*

5. Soft color interactions

The rapidity gaps in the diffractive interactions are explained in the discussed models by the color singlet, vacuum exchange – the pomeron, being a complicated gluon exchange interaction. The basic assumption in the soft color interaction model [23] is that the underlying hard interaction of a diffractive event is the same as in a typical DIS event. Thus, the flatness of the ratio $\sigma^{diff}/\sigma^{tot}$ in both x and Q^2 is a natural consequence of this model. The color singlet exchange responsible for the rapidity gap is the result of soft interactions which rearrange color of the final state partons without affecting their momenta, see Fig. 7. This leads to a region in phase space without string in the Lund model of hadronization, which leads to the rapidity gap. Such a reshuffling in color space was implemented in the Monte Carlo event generators, providing good description of the diffractive data in DIS.

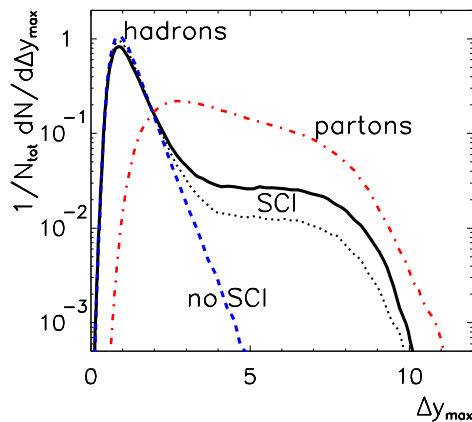


Figure 8. *Distribution of events with maximal rapidity gap Δy_{max} in DIS events (reproduced from [23]).*

In Fig. 8 the distribution of events with maximal rapidity gap Δy_{max} is shown, using Monte Carlo models with and without the soft color interactions (SCI). As we see, without SCI large rapidity gaps are exponentially suppressed. This is not the case for SCI. In summary, in the presented approach the rapidity gap formation is a final state soft effect which is not connected to the hard scattering process.

6. Summary

The unexpectedly large fraction of diffractive DIS events observed at HERA renewed an interest in diffractive phenomena in high energy scattering, now in the context of perturbative QCD. We presented three approaches to the generation of rapidity gaps which are not exponentially suppressed. In the first one, somewhat conventional pomeron mechanism, known from the Regge approach to high energy scattering, was supplemented by hard structure which emerges in the experimentally observed diffractive events. In the second approach, DIS diffraction is strongly related to the necessity to take into account unitarization effects in the QCD description of color singlet gluonic exchanges. In the third approach, the difference between the normal and diffractive DIS events lies in the final state soft interactions which are decoupled from the hard part of the final parton state. All these description could be tested for more exclusive diffractive processes, e.g. in vector meson or large- p_T jet production in DIS and in hadron-hadron collisions. For more details on hard diffraction, we refer to the excellent reviews [7, 24].

ACKNOWLEDGEMENTS

A partial support of the Polish State Committee for Scientific Research, grant no. 1 P03B 028 28, is acknowledged.

REFERENCES

1. H1 Collaboration, C. Adloff *et al.*, *Z. Phys.* **C76** (1997) 613.
2. ZEUS Collaboration, M. Derrick *et al.*, *Eur. Phys. J.* **C6** (1999) 43.
3. ZEUS Collaboration, S. Chekanov *et al.*, *Eur. Phys. J.* **C38** (2004) 43.
4. UA8 Collaboration, R. Bonino *et al.*, *Phys. Lett.* **B211** (1988) 239.
5. J. C. Collins, *Phys. Rev.* **D57** (1998) 3051, Erratum-*ibid.* **D61** (2000) 019902.
6. J. C. Collins, L. Frankfurt and M. Strikman *Phys. Lett.* **B307** (1993) 161.
7. M. Wüsthoff and A. D. Martin, *J. Phys.* **G25** (1999) R309.
8. A. Berera and D.E. Soper, *Phys. Rev.* **D53** (1996) 6162.
9. F. Hautmann, Z. Kunszt and D. E. Soper, *Phys. Rev. Lett.* **81** (1998) 3333; *Nucl. Phys. Proc. Suppl.* **79** (1999) 260.
10. G. Ingelman and P. Schlein, *Phys. Lett.* **B152**, 256 (1985).
11. A. Donnachie and P. V. Landshoff, *Nucl. Phys.* **B 231** (1984) 189.
12. K. Golec-Biernat and J. Kwieciński, *Phys. Lett.* **B353**, 329 (1995).
13. K. Golec-Biernat and J. Kwieciński, *Phys. Rev.* **D55** (1997) 3209; K. Golec-Biernat, J. Kwieciński and A. Szczurek, *Phys. Rev.* **D56** (1997) 3955.
14. N. N. Nikolaev and B. G. Zakharov, *Z. Phys.* **C49** (1991) 607; *Z. Phys C* **53** (1992) 331.

15. L. N. Lipatov, *Sov. J. Nucl. Phys.* **23** (1976) 338; E. A. Kuraev, L. N. Lipatov and V. S. Fadin, *Sov. Phys. JETP* **44** (1976) 443; *ibidem.* **45** (1977) 199; Ya. Ya. Balitsky and L. N. Lipatov, *Sov. J. Nucl. Phys.* **28** (1978) 338.
16. L. V. Gribov, E. M. Levin and M. G. Ryskin, *Phys. Rep.* **100** (1983) 1.
17. K. Golec-Biernat and M. Wüsthoff, *Phys. Rev.* **D59** (1999) 014017;
18. K. Golec-Biernat and M. Wüsthoff, *Phys. Rev.* **D60** (1999) 114023.
19. A. M. Staśto, K. Golec-Biernat and J. Kwieciński, *Phys. Rev. Lett.* **86**, 596 (2001).
20. E. Iancu and R. Venugopalan, hep-ph/0303185.
21. J.R. Forshaw, R. Sandapen and G. Shaw, *Phys. Lett.* **B594** (2004) 283.
22. K. Golec-Biernat and M. Wüsthoff, *Eur. Phys. J.* **C20**, 313 (2001).
23. S. J. Brodsky, R. Enberg, P. Hoyer and G. Ingelman, hep-ph/0409119, and references therein.
24. A. Hebecker, *Phys. Rep.* **331** (2000) 1; *Acta Phys. Polon.* **B30** (1999) 3777.